ENgineered Nanoparticle Impact on Aquatic Environments: Structure, Activity and Toxicology

Contract Agreement: NMP4-SL-2009-229244

Website: http://www.ennsatox.eu

Coordinator: Professor Andrew Nelson, Centre for Molecular Nanoscience (CMNS), School of Chemistry, University of Leeds, UK

1. Consortium Members

No.	Beneficiary Name	Short Name	Country
1 (coordinator)	University of **Leeds**	UNIVLEEDS	UK
2	**Wageningen** University	WU	Netherlands
3	University of **Antwerp**	UA	Belgium
4	Stazione Zoologica **Anton Dohrn**	SZN	Italy
5	**Lleida** University	UdL	Spain
6	**Marine Biological Association** of UK	MBA	UK
7	Society of Environmental Toxicology And Chemistry (**SETAC**) – Europe	SETAC	Belgium

2. Project Title

ENgineered Nanoparticle Impact on Aquatic Environments: Structure, Activity and Toxicology

3. Acronym

ENNSATOX

4. Project Start and End Dates

Start date: 1st July 2009

End date: 30th June 2012

Duration: 36 months

5. Project Budget

€3,655,316 Total Budget

€2,816,500 EC Contribution

6. Abstract

The use of engineered nanoparticles (NP) in cosmetics, pharmaceuticals, sensors and many other commercial applications has been growing exponentially over the past decade. EU and Member States' research into the environmental impact of these materials, particularly in aquatic systems, is at an early stage. There is a large uncertainty into the environmental risk posed by these new materials. ENNSATOX addresses this deficit through a comprehensive investigation relating the structure and functionality of well characterised engineered nanoparticles to their biological activity in environmental aquatic systems. ENNSATOX takes account of the impact of nanoparticles on environmental systems from the initial discharge to the uptake by organisms. Accordingly an integrated approach will assess the activity of the particles in a series of biological models of increasing complexity. Parallel environmental studies will take place on the behaviour of the nanoparticles in natural waters and how they modify the particles' chemical reactivity, physical form and biological activity. A comprehensive theoretical model will be developed describing the environmental system as a series of biological compartments where particles transport between a) compartments by advection-diffusion and b) between phases by a transfer function. Following optimisation of the transfer functions a generic predictive model will be derived for the environmental impact of each class of nanoparticle in aqueous systems. The project will include the use of unique biological membrane models not only to understand better the interaction of nanoparticles with cell membranes from an organism health point of view but also to develop suitable nanoparticle screening procedures which can substitute for the more lengthy *in vivo* tests. ENNSATOX will generate: 1) Exploitable IP of screening devices and simulation software; 2) Set of standard protocols; 3) Global dissemination of results; 4) Creation of an EU laboratory service; 5) Tools and data to inform EU Regulation; 6) Risk assessment procedures.

7. Project Logo and Website

Logo: ennsatox NANOPARTICLES IN THE AQUATIC ENVIRONMENT

Website: www.ennsatox.eu

8. Graphical Elements which Illustrate the ENNSATOX Project

Figure A. Typical Characterisation Results - TEM Bright field image of ZnO nanoparticles on a holey carbon film and in-house polyol ZnO synthesis.

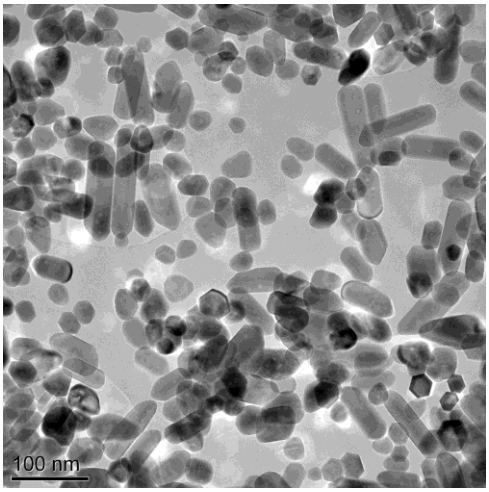

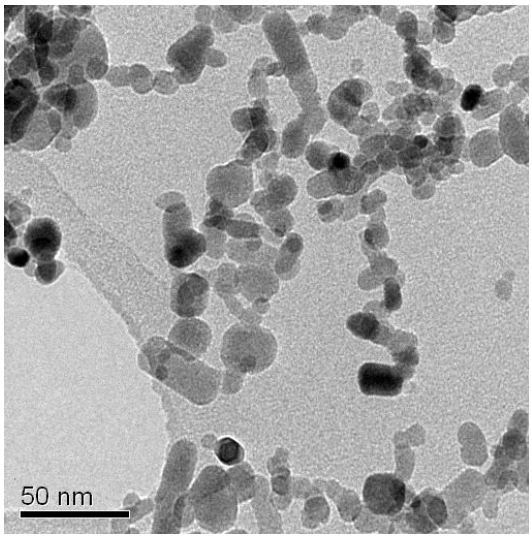

Figure B. Schematic representation of the *diffusion-adsorption-internalization* model. Uptake is described through the following sequential steps: a) diffusion of NPs from bulk solution (***blue***); b) reversible adsorption/desorption of NPs on the biomembrane following a Langmuir-like kinetics (***red***); c) internalization of NPs through endocytosis or similar mechanisms (***purple***); and, finally, d) efflux of NPs out of the organism (***green***).

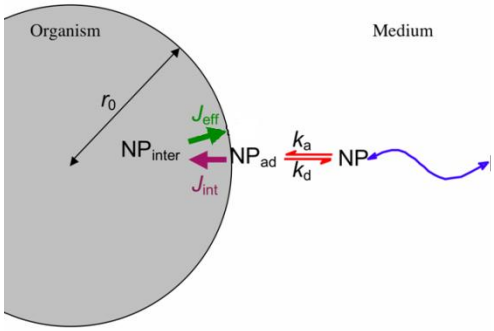

Figure C. The ENNSATOX Nanosensor for NP biomembrane activity.

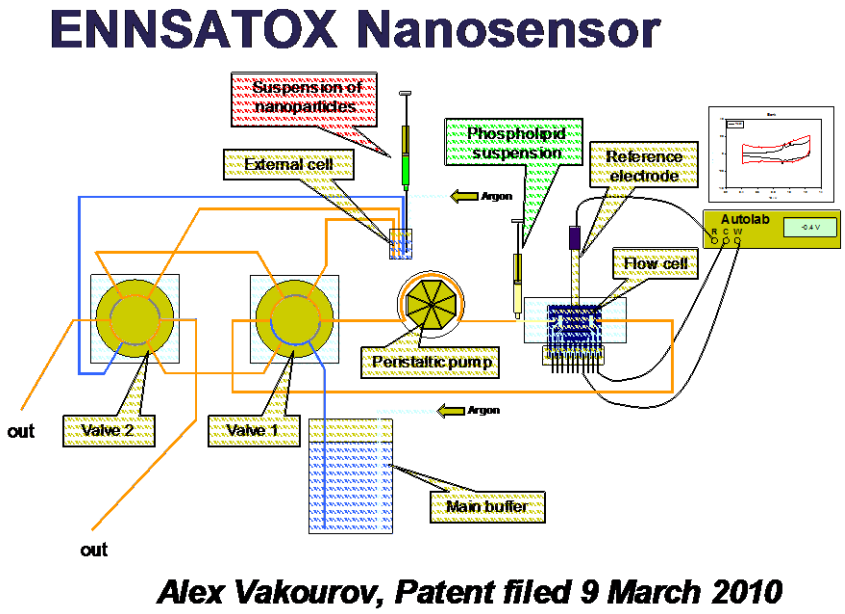

Figure D. Evidence that SM30 silica NPs are entering the cytoplasm cells at 4^{o}C by adhering to and becoming wrapped in the membrane – this is a passive uptake mechanism as normal endocytosis should be inactive at this temperature.

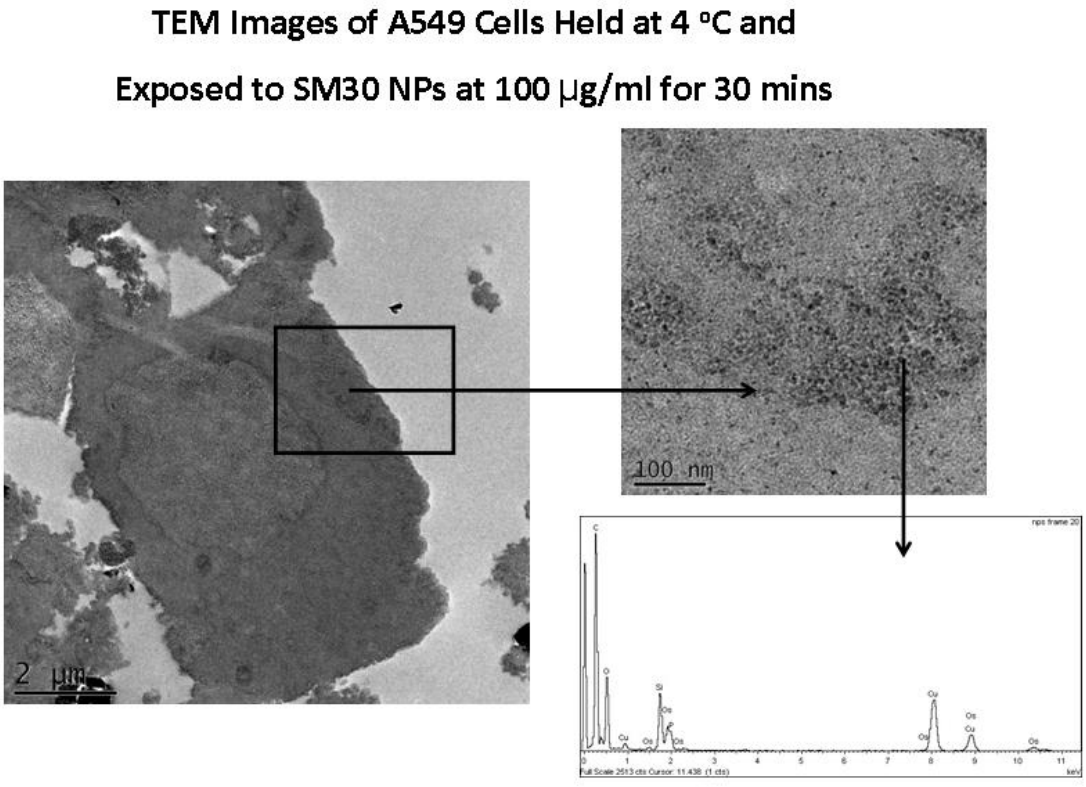

9. ENNSATOX Consortium Contacts

First Name	Last Name	Affiliation	Address	E-mail
Nathalie	**Adam**	Universiteit Antwerpen	Ecophysiology, Biochemistry and Toxicology, Groenenborgerlaan 171 - U537, B-2020 Antwerp, Belgium	nathalie.adam@ua.ac.be
Dave	**Arnold**	SETAC Europe	Avenue de la Toison d'Or 67, B-1060 Brussels, Belgium	dave.arnold@setac.org
Ronny	**Blust**	Universiteit Antwerpen	Department of Biology, Groenengorgerlaan 171, B-2020 Antwerp, Belgium	ronny.blust@ua.ac.be
Andy	**Brown**	University of Leeds	Institute for Materials Research, SPEME, Leeds LS2 9JT, UK	a.p.brown@leeds.ac.uk
Euan	**Brown**	Stazione Zoologica Anton Dohrn	Animal Physiology and Evolution, Villa Comunale, Napoli 80121, Italy	brown@szn.it
Rik	**Brydson**	University of Leeds	Institute for Materials Research, SPEME, Leeds LS2 9JT, UK	mtlrmdb@leeds.ac.uk
Roel	**Evens**	SETAC Europe	Avenue de la Toison d'Or 67, B-1060 Brussels, Belgium	roel.evens@setac.org
Josep	**Galceran**	Universidad de Lleida	Departament de Quimica, Alcalde Rovira Roure, Lleida 25198, Spain	galceran@quimica.udl.cat
Alistair	**Hay**	University of Leeds	Molecular Epidemiology Unit, Leeds Institute for Genetics, Health and Therapeutics Laboratories, School of Medicine, Leeds LS2 9JT, UK	a.w.m.hay@leeds.ac.uk
Lars	**Jeuken**	University of Leeds	School of Physics and Astronomy, EC Stoner Building, Leeds LS2 9JT, UK	l.j.c.jeuken@leeds.ac.uk
Mieke	**Kleijn**	Wageningen University	Laboratory of Physical Chemistry and Colloid Science, P.O. Box 8038, 6700 EK, The Netherlands	mieke.kleijn@lwur.nl
Bill	**Langston**	Marine Biological Association	Citadel Hill, Plymouth PL1 2PB, UK	wjl@mba.ac.uk
Frans	**Leermakers**	Wageningen University	Laboratory of Physical Chemistry and Colloid Science, P.O. Box 8038, 6700 EK, The Netherlands	frans.leermakers@wur.nl
Steve	**Milne**	University of Leeds	Institute for Materials Research, SPEME, Leeds LS2 9JT, UK	s.j.milne@leeds.ac.uk
Andrew	**Nelson (Coordinator)**	University of Leeds	CMNS, School of Chemistry, Leeds, LS2 9JT, UK	a.l.nelson@leeds.ac.uk
Nick	**Pope**	Marine Biological Association	Citadel Hill, Plymouth PL1 2PB, UK	ndpo@MBA.ac.uk

First Name	Last Name	Affiliation	Address	E-mail
Jaume	**Puy**	Universidad de Lleida	Departament de Quimica, Alcalde Rovira Roure, Lleida 25198, Spain	jpuy@quimica.udl.cat
Carlos	**Rey-Castro**	Universidad de Lleida	Departament de Quimica, Alcalde Rovira Roure, Lleida 25198, Spain	carlos.rey@quimica.udl.cat
Michael	**Routledge**	University of Leeds	Molecular Epidemiology Unit, Leeds Institute for Genetics, Health and Therapeutics Laboratories, School of Medicine, Leeds LS2 9JT, UK	m.n.routledge@leeds.ac.uk
Claudia	**Schmitt**	Universiteit Antwerpen	Ecophysiology, Biochemistry and Toxicology, Groenenborgerlaan 171 - U.731, B-2020 Antwerp, Belgium	claudia.schmitt@ua.ac.be
Karen	**Steenson (*Project Manager*)**	University of Leeds	CMNS & Faculty of Engineering, Leeds LS2 9JT, UK	k.a.steenson@leeds.ac.uk
Herman	**van Leeuwen**	Wageningen University	Laboratory of Physical Chemistry and Colloid Science, P.O. Box 8038, 6700 EK, The Netherlands	herman.vanleeuwen@wur.nl

Please note that the figures below correspond to those quoted in the Final Report.

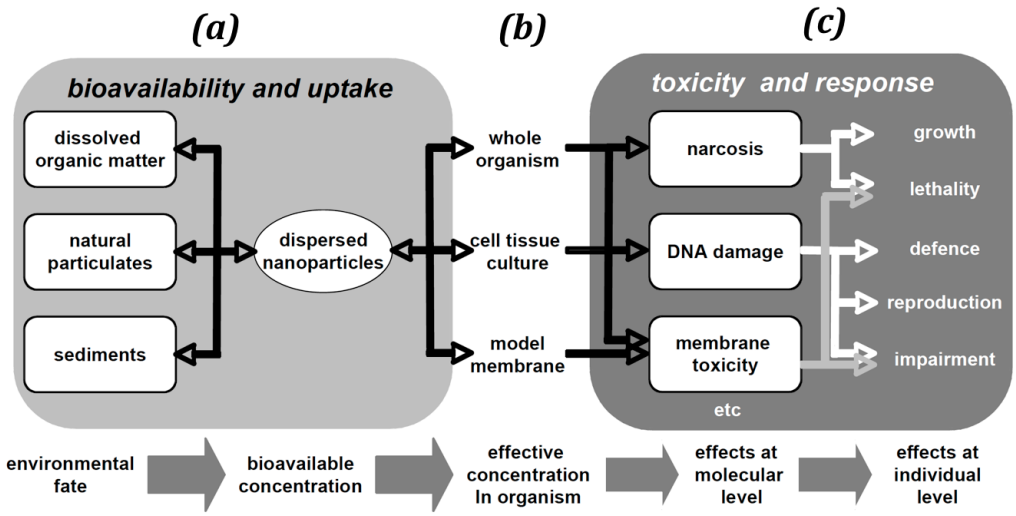

Figure 1: above sets the above objectives and activities in an integrated strategic environmental framework. The figure shows the environmental discharge and behaviour of the nanoparticles in the left hand compartment ***(a)*** *and, the impact of nanoparticles on the biological barriers in between the two compartments* ***(b)*** *and on the aquatic organisms in the right hand compartment* ***(c)****.*

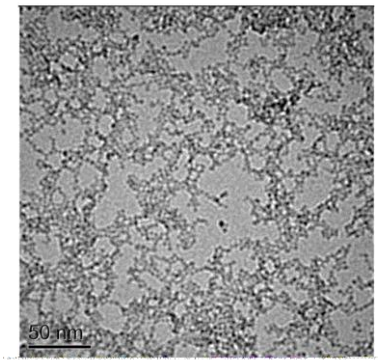

Figure 2. TEM image of in-house synthesised ZnO nanoparticles dried from fresh water suspension

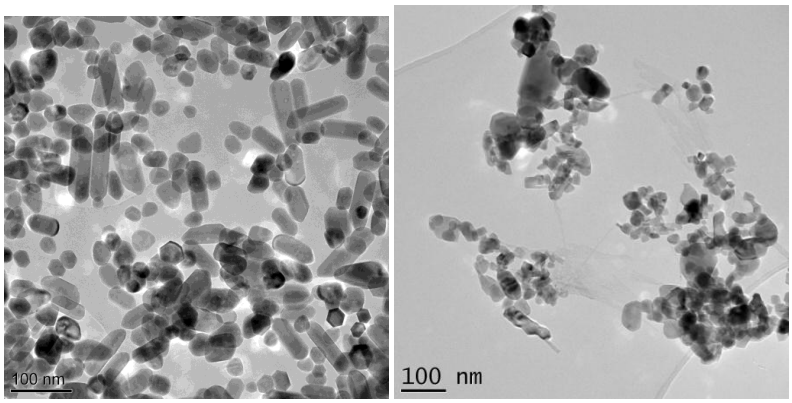

Figure 3: In-house polyol ZnO synthesis vs Commercial ZnO powder

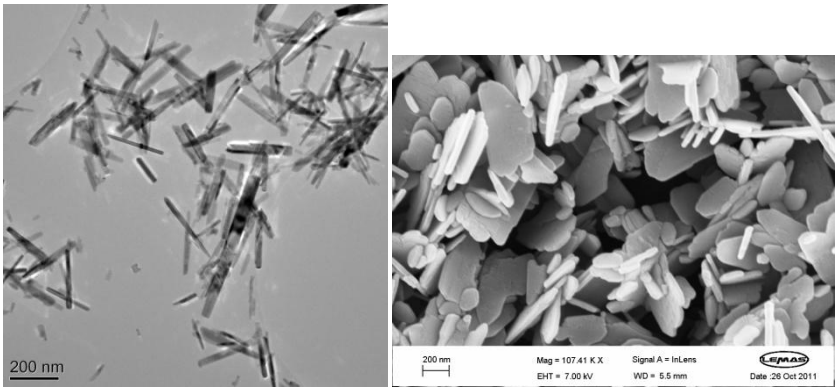

Figure 4: Example of EN-Z-7 vs Example of EN-Z-9

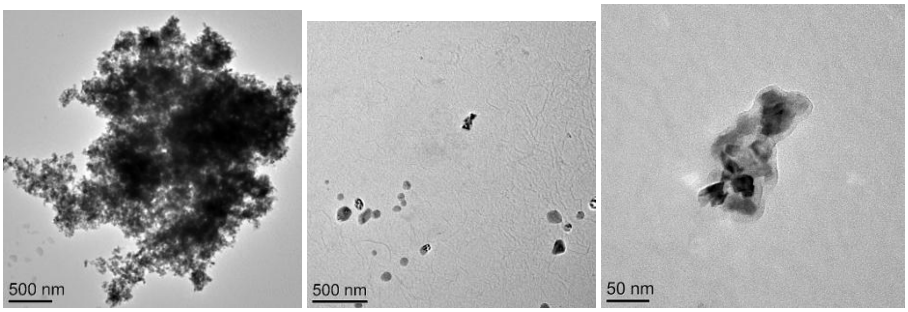

Figure 5: ZnO suspension (BSA-DMEM-Water) prepared by (left)drop casting technique (middle) plunge freezing technique. (right) High magnification TEM image showing the BSA coating (protein corona) on the nanoparticles.

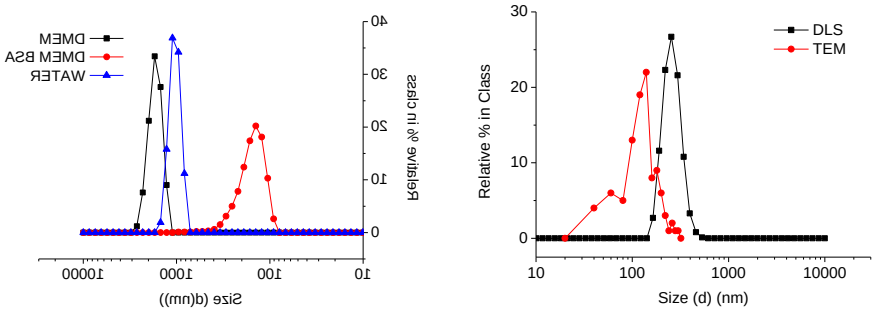

Figure 6: DLS plot showing size distribution for ZnO suspended in (i) distilled water, (ii) DMEM-Water and (iii) DMEM+Water+BSA and (b) DLS number plot (i) for colloidal dispersion of ZnO nanoparticles (DMEM+Water+BSA) with TEM plunge freezing data (ii) overlaid.

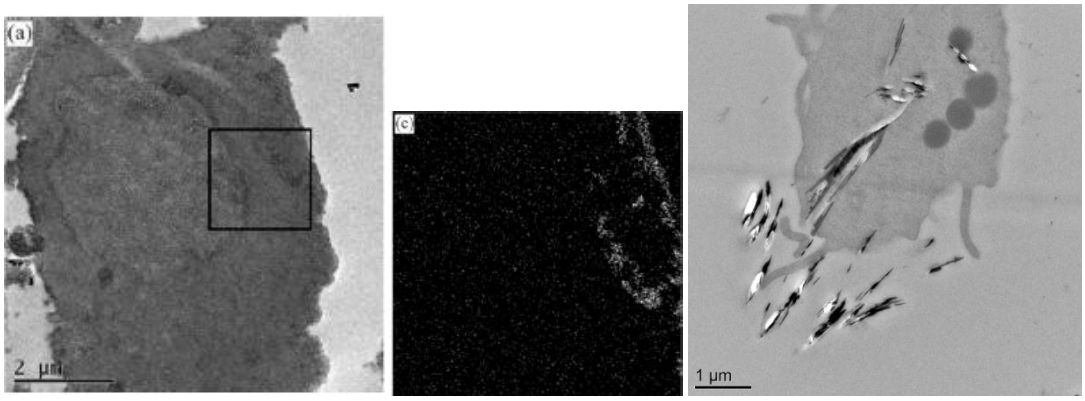

Figure 7: On left image of EN-S-1.3 in A549 cells exposed at 4 ^{o}C to 100 mg per mL for 30 mins. Image in middle is STEM Si X-ray map highlighting the location of the silica NPs (bright contrast in the map) in the cell within the boxed region in left image. On right image of EN-Z-7 needles in A549 cells exposed to 1mg per mL for 6 hours.

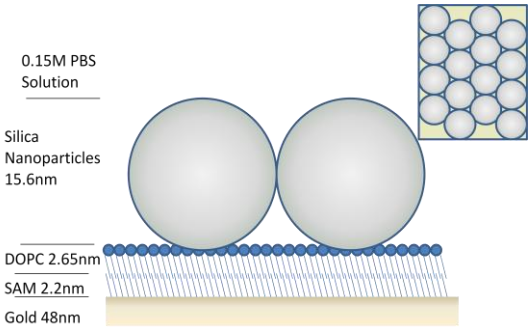

Figure 8: Shows schematic of nanoparticle adsorption on layers of lipid (DOPC), self-assembled monolayer (octadecanethiol) and gold surface. Inset: top-down view showing theoretical close-packed nanoparticle arrangement, with 0.6046 layer volume.

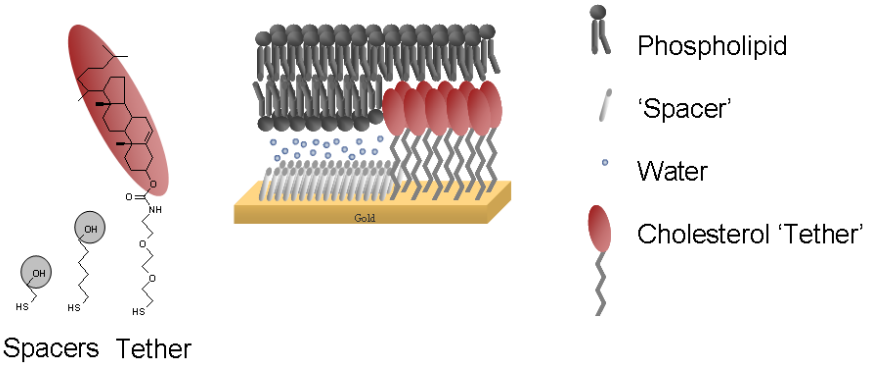

Figure 9: Shows examples of supported phospholipid membranes used for toxicity assay of nanoparticles dispersions.

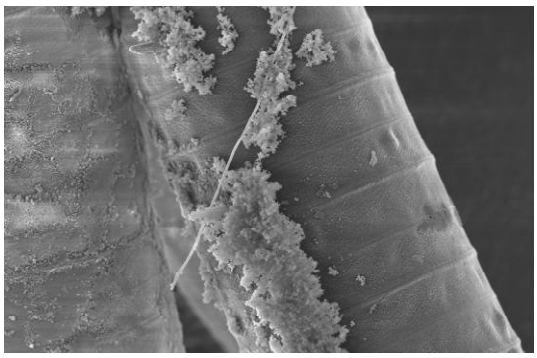

Figure 10: Shows Oscillatoria princeps incubated with SiO2. Cells separated by septa (arrowed). Right filament partially covered by SiO2, left filament completely covered.

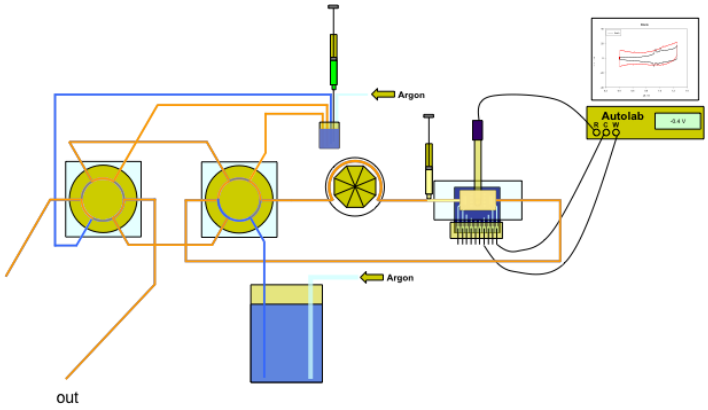

Figure 11: Schematic of the ENNSATOX nanosensor for high throughput assay of biomembrane activity of nanoparticle dispersions.

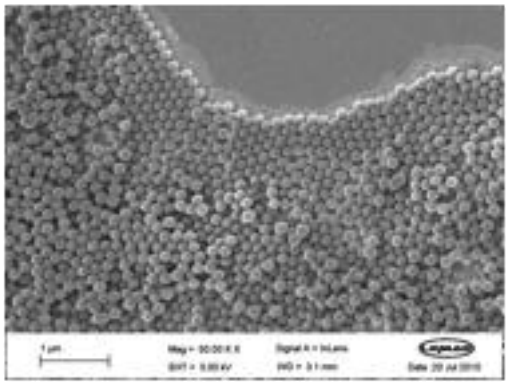

Figure 12: Scanning electron microscopy (SEM) images of phospholipid monolayer coated Pt/Hg film electrode after incubation with 175 nm AngstromSphere silica.

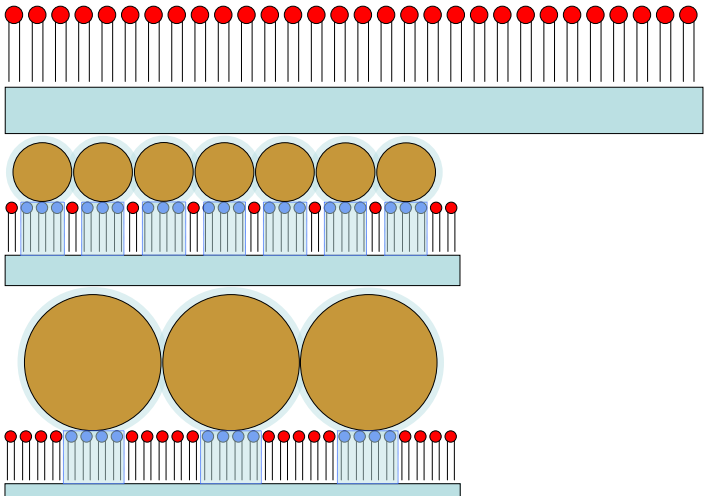

Figure 13: Schematic view of silica nanoparticles interaction with phospholipid domain. (TOP) phospholipid monolayer on mercury surface, (MIDDLE) small nanoparticles on phospholipid monolayer, (BOTTOM) large nanoparticles on phospholipid monolayer. Blue represents domains of DOPC with surface within interfacial layer and red represents domains of DOPC with surface outside interfacial layer.

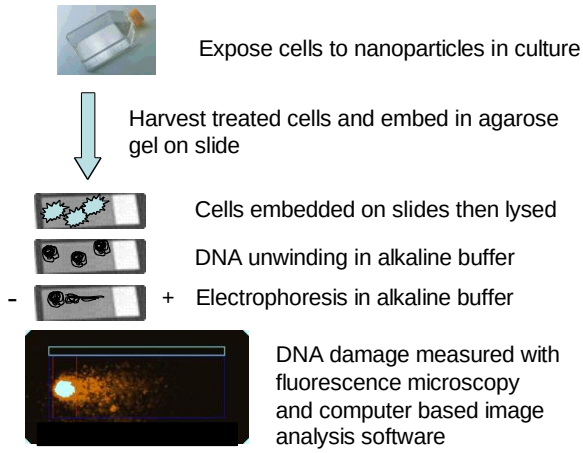

Figure 14: Shows the Comet assay protocol being used to assess nanoparticle dispersions' activity.

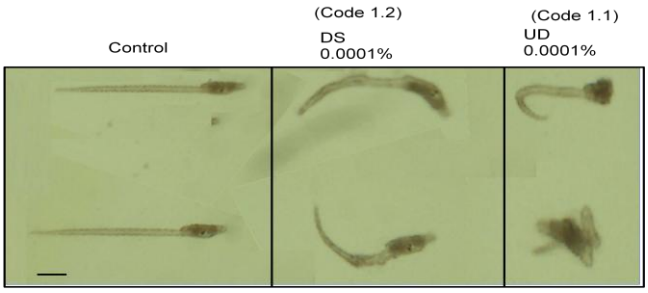

Figure 15: Developmental assays. Ludox SM30 SiO_2 (Dialysed, DS left and undialysed, UD right) NPs diluted 1 in 100 in sterile filtered natural seawater ,1 x 10^{-6} sperm mL^{-1} added to media then after 5 minutes media added to eggs. Note the developmental problems with the NP exposed larvae.

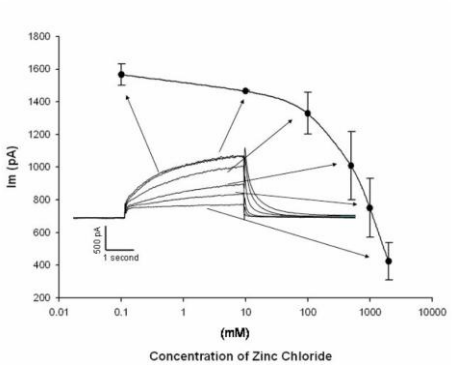

Figure 16: Dose response of hERG peak currents in various concentrations of Zn^{2+}. The EC_{50} of Zn^{2+} on hERG is estimated to be of the order of 1 mM. The results represent the mean and standard deviation of results from at least five experiments.

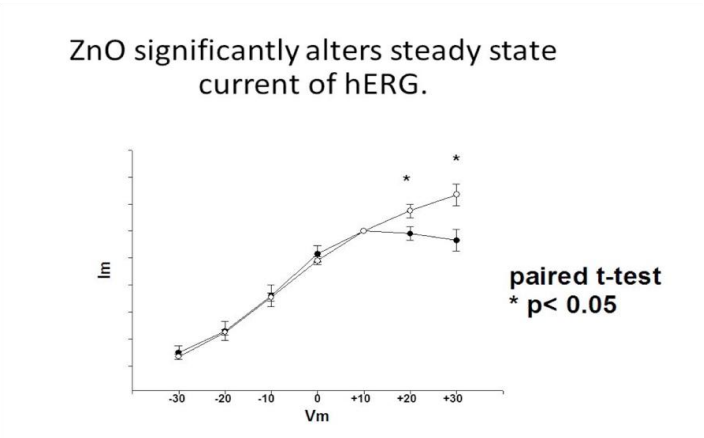

Figure 17: ZnO removes the fast inactivation of hERG and is so doing increases the amplitude of the current at positive voltages. The graph shows the extracted values for current voltage relations of the steady state K^+ current under different voltage steps.

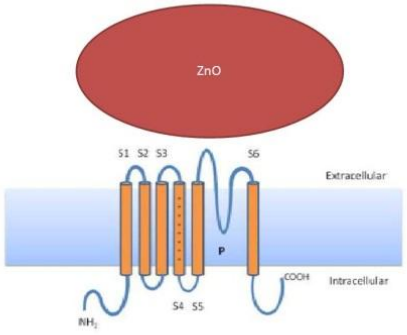

Figure 18: A simple model to explain the interaction between ZnO NPs and hERG.

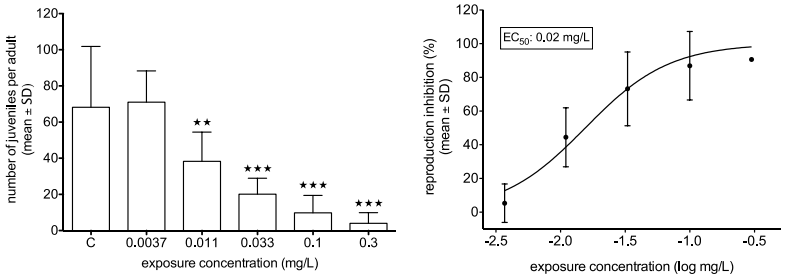

Figure 19: Chronic toxicity of ZnO nanodispersion on the reproduction of Daphnia magna (mean ± SD) after 21 days of exposure. Number of juveniles per adult Daphnia; one-way ANOVA with Dunnet's post test, significant differences p < 0.001-0.01 (left) and sigmoidal dose-response curve on the inhibition of reproduction (right).

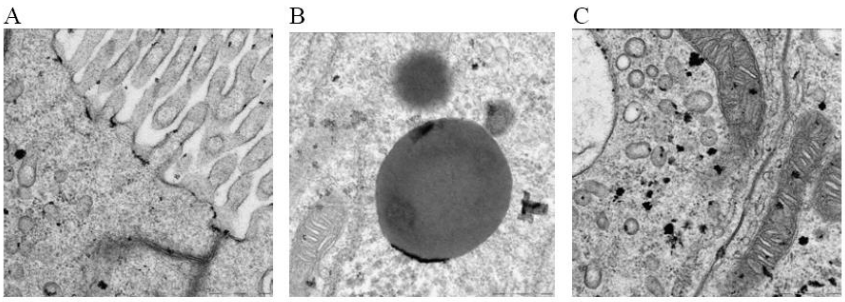

Figure. 20: Feeding the animals with ZnO nanoparticles results in an accumulation of the particles in the stomach tissue. TEM analysis of this organ indicates that nanoparticles, found at the plasma membrane of the cells facing the lumen, pass into the cytoplasm and through the junctions (A). Clusters of ZnO nanoparticles can be observed at the edge of zymogen granules (B), in the mitochondria and scattered in the cytoplasm (C). Scale bars 0.5 µm.

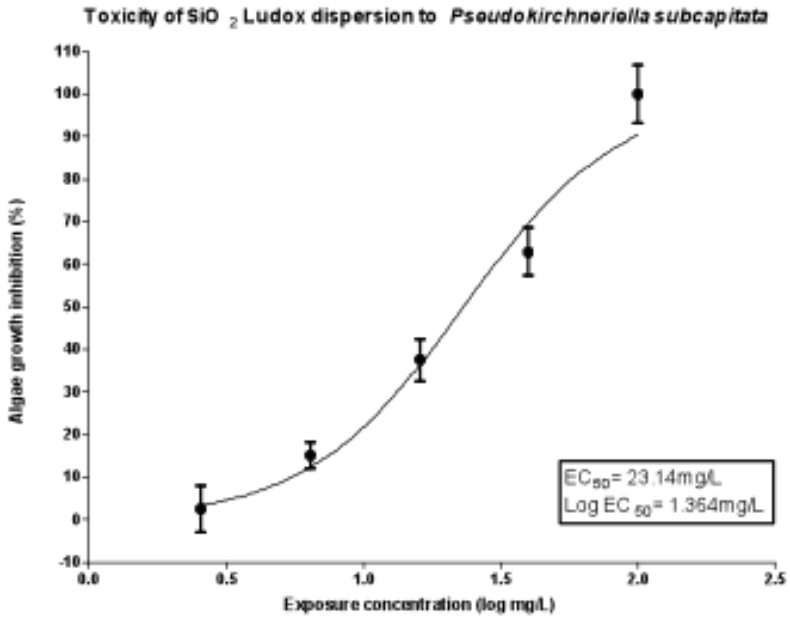

Figure 21: Toxicity of SiO_2 Ludox dispersion to the algae species Pseudokirchneriella subcapitata. On the X-axis the exposure concentration (2.56, 6.4, 16, 40, 100 mg L^{-1}) is indicated as a log-scale, whereas on the Y-axis the toxicity is indicated as the percentage of growth inhibition caused by the dispersion.

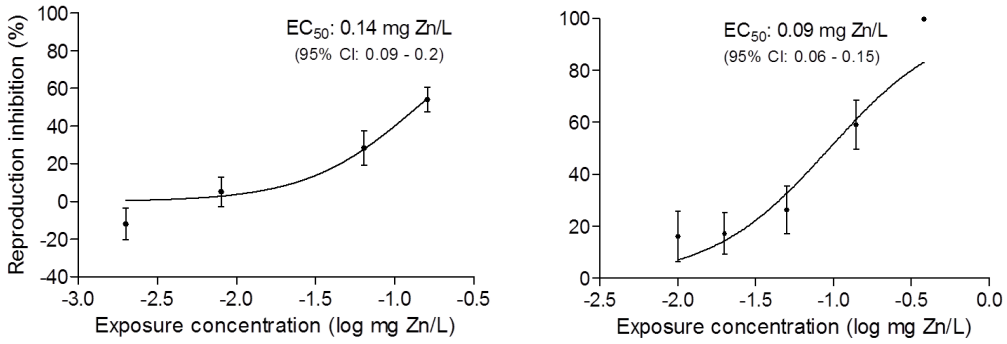

Figure 22: The chronic toxicity of ZnO nanosun (left) and $ZnCl_2$ (right) to the reproduction of Daphnia magna after 21 days. X-axis: exposure concentration (log mg Zn/L), Y-axis: Reproduction inhibition (%).

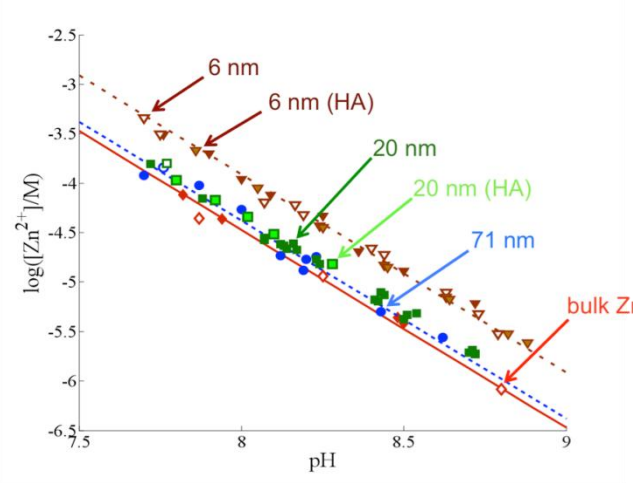

Figure 23: Equilibrium concentration of Zn^{2+} ions in ZnO NP dispersions prepared in 0.1M KCl (solid symbols) or 0.1 M KNO_3 (open symbols) at 25ºC, measured by AGNES. Light green and light brown markers indicate values measured in the presence of 50 mg/L of humic acid. Lines: model correlation with pH and primary particle size, using γ =0.32 J/m^2.

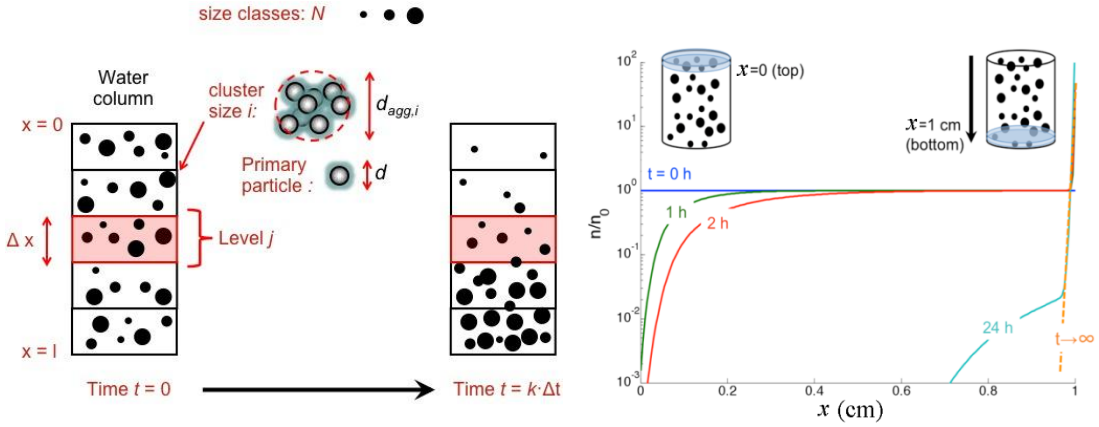

Figure 24: Left: Schematic representation of the discretised transport model. Right: Time evolution of the average concentration profile of monodisperse NPs (d_{agg} = 650 nm) in a well, estimated by the diffusion-sedimentation model. n/n_0 is the normalized (with respect to the original solution) number of particles at a certain height.

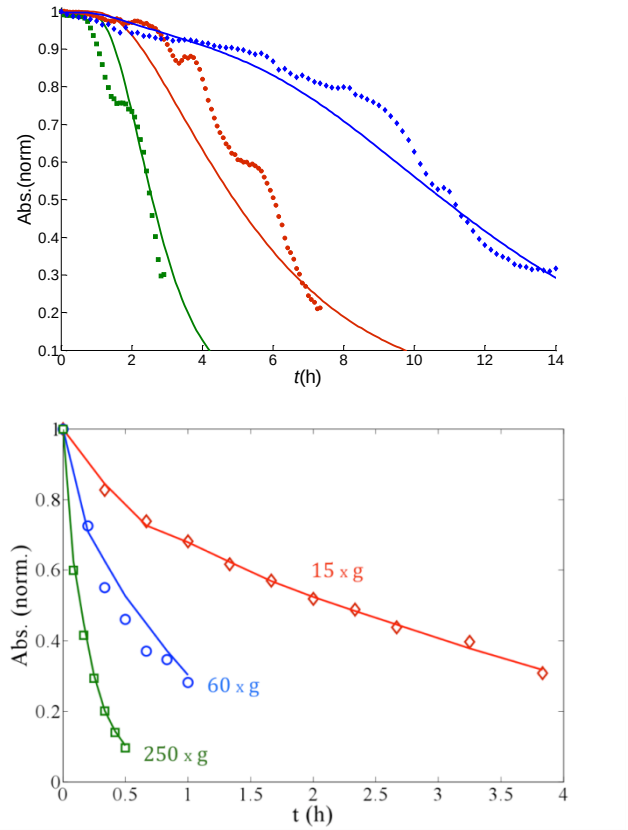

Figure 25: UV-vis measurements of the fraction of ZnO NPs remaining in supernatant (0.1M KNO_3 and 5 mg HA /L). Left: settling of 71 nm NPs having d_{agg}= 250 nm (blue), 650 nm (red), and 1000 nm (green). Right: centrifugation of 20 nm NPs with d_{agg}= 130 nm at different rotor speeds (parameter a). The lines correspond to the theoretical expectations of the model when fitting the size distribution and the fractal dimension of the aggregate.

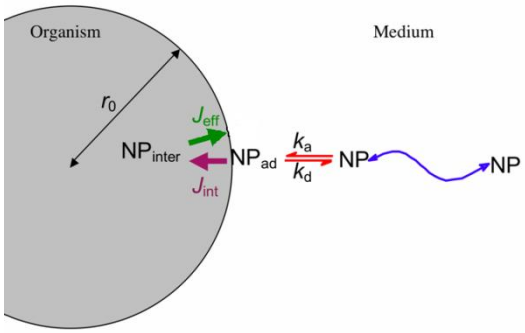

Figure 26: Schematic representation of the diffusion-adsorption-internalization model. Uptake is described through the following sequential steps: a) diffusion of NPs from bulk solution (blue); b) reversible adsorption/desorption of NPs on the biomembrane following a Langmuir-like kinetics (red); c) internalization of NPs through endocytosis or similar mechanisms (purple); and finally d) efflux of NPs out of the organism (green).

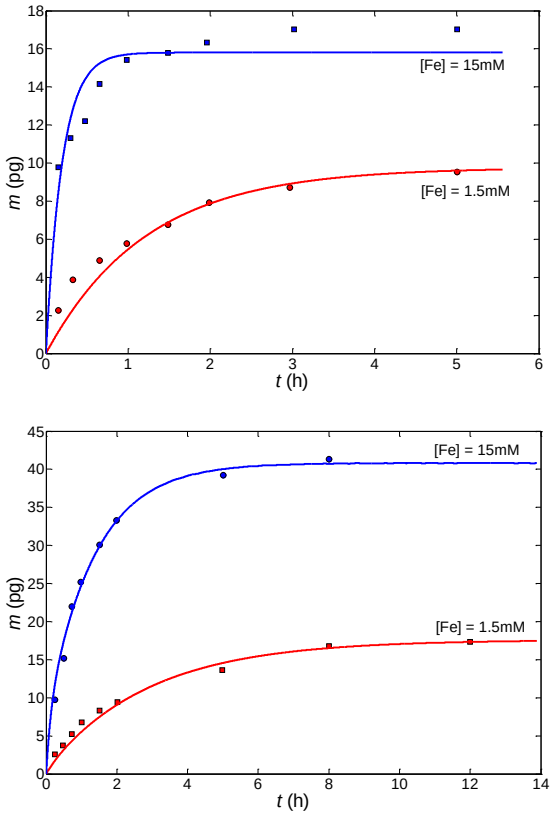

Figure 27: Fitting of the diffusion-adsorption-internalization model to experimental uptake data of magnetite Fe_2O_3 NPs (diameter 8.7nm) in HeLa cells (diameter 20.2 µm) incubated at 4ºC (left) and 37ºC (right).

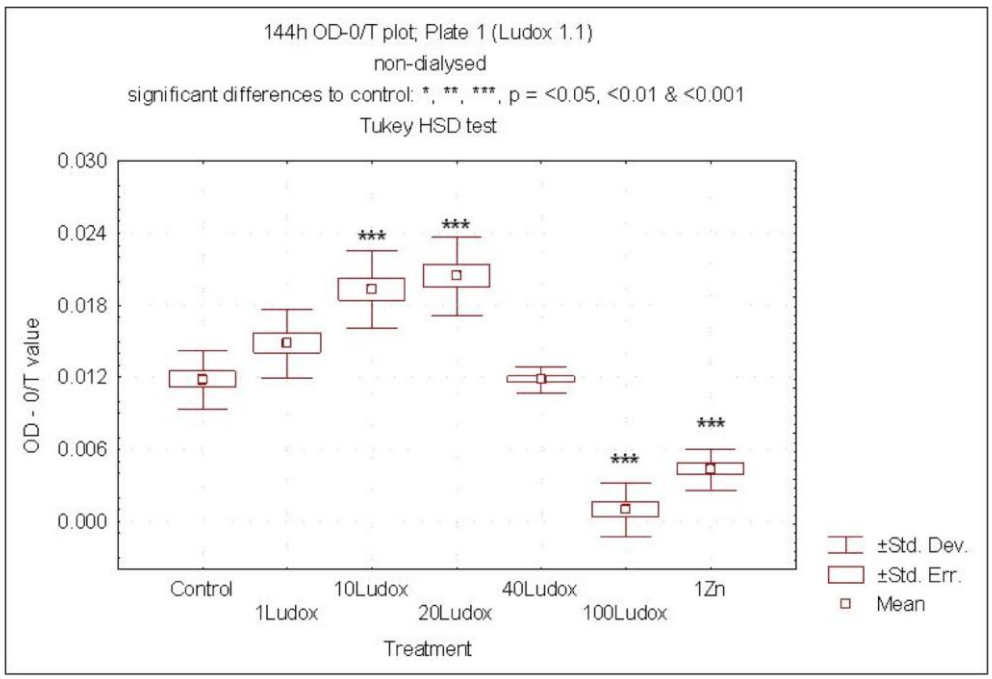

Figure 28: Isochrysis galbana. Growth (measured as absorbance at 440nm – absorbance at 750nm) after a 6 day period of exposure to SM30 as mg L^{-1} LUDOX, relative to controls (including positive control of 1 mg L^{-1} Zn^{2+} as zinc sulphate).

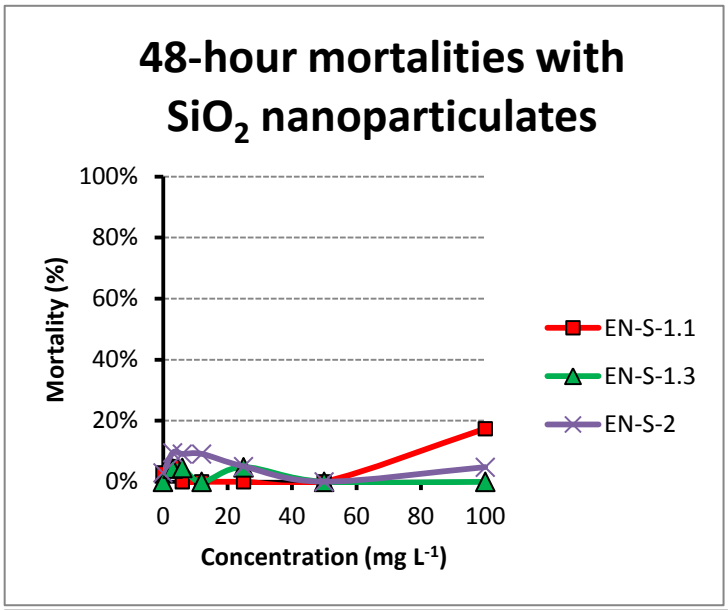

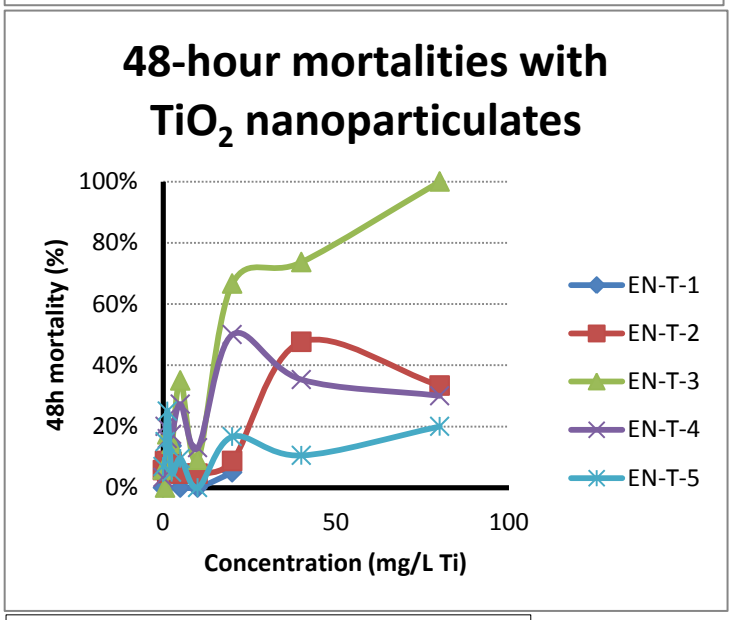

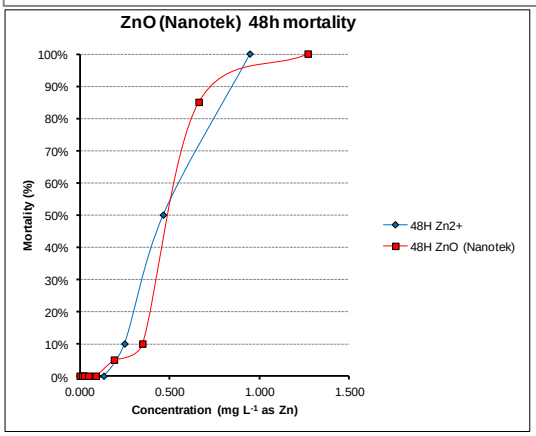

Figure 29: Tisbe battagliai 48-hour mortalities during exposure to SiO_2 nanoparticulate materials in seawater.

Figure 30: Tisbe battagliai 48-hour mortalities during exposure to TiO_2 nanoparticulate materials in seawater.

Figure 31: Tisbe battagliai. Lethality curves for Nanotek ZnO nanoparticulates. Zn^{2+} toxicity is shown for comparison.